Journal of Porous Materials (2019) 26:281–290
https://doi.org/10.1007/s10934-018-0654-8

Facile synthesis of porous anionic hydrogel embedded with nickel nanoparticles and evaluation of its catalytic performance for the rapid reduction of 4-nitrophenol

Muhammad Ajmal[1] · Faiza Aftab[2] · Iram Bibi[2] · Muzaffar Iqbal[3] · Jaweria Ambreen[4] · Hafiz Badaruddin Ahmad[5] · Naeem Akhtar[5] · Abdul Haleem[6] · Muhammad Siddiq[7]

Published online: 27 July 2018

Abstract
Anionic hydrogel was prepared by free radical copolymerization of acrylamide and acrylic acid. The anionic groups acted as adsorption sites to load Ni(II) ions and the subsequent reduction of loaded Ni(II) ions into nanoparticles enabled the prepared hydrogels to act template for the preparation of nanostructured Ni particles. The characteristics of the prepared hydrogel and hydrogel–nickel nanoparticle composite were studied with Fourier transform infrared spectroscopy, transmission electron microscopy, thermal gravimetric analysis, X-ray photoelectron spectroscopy and X-ray diffraction technique. Swelling behaviour of hydrogel in aqueous medium was analysed by gravimetric analysis. Catalytic performance of the prepared poly(acrylamide-*co*-acrylic acid)–nickel nanoparticle hydrogel composite was investigated in the reduction of 4-nitrophenol (4-NP). Effects of temperature and catalyst dose on the reduction rate were also studied. Activation energy (E_a) for the reduction of 4-NP was found to be 43.46 kJ/mol. A maximum reduction rate of 0.40 min^{-1} was observed at room temperature.

Keywords Porous hydrogel · Ni nanoparticles · Catalysis · 4-Nitrophenol

1 Introduction

Owing to their high degree of porosity, tunable chemical and three dimensional physical structures and good mechanical strength, development of hydrogels has gained a lot of interest of the people working on material science. Hydrogels are very soft materials having high water contents. They are generally prepared from hydrophilic polymers which are cross-linked with each other. Hydrophilicity of hydrogels can be controlled by controlling the degree of cross-linking and amount of monomers having hydrophilic and/or hydrophobic nature. These hydrophilic materials have attracted a great deal of interest in controlled and targeted delivery of drugs [1], engineering of tissues [2], biomedical implants [3], purification of contaminated water [4], enhanced oil recovery [5] synthesis and stabilization of inorganic nanoparticles [6–10], and bionanotechnology [11]. Hydrogels exhibit this broad spectrum of applications because of having tunable physical and chemical characteristics and their environmental friendly nature [12]. Recently, development of hydrogel composites with nano-sized inorganic materials has become a fascinating art in order to increase the applicability of hydrogels. Hydrogels are widely applied

✉ Muhammad Siddiq
m_sidiq12@yahoo.com

1 Department of Chemistry, University of Wah, Quaid Avenue, Wah Cantt., Rawalpindi 47040, Pakistan

2 Department of Chemistry, Hazara University, Garden Campus, Mansehra, NWFP, Pakistan

3 National Centre for Nanoscience and Technology, University of Chinese Academy of Sciences, Beijing 100190, China

4 Department of Physics, Comsats Institute of Information Technology, Chak Shahzad, Park Road, Islamabad 45550, Pakistan

5 Institute of Chemical Science, Bahauddin Zakariya University, Multan 60800, Pakistan

6 CAS Key Laboratory of Soft Matter Chemistry, Department of Polymer Science and Engineering, University of Science and Technology of China, Hefei 230026, Anhui, China

7 Department of Chemistry, Quaid-I-Azam University, Islamabad 45320, Pakistan

as reactors for the preparation and stabilization of metal nanoparticles. Depending upon composition, hydrogels contain metal-binding functional groups such as $–SO_3H$, –COOH, –OH, $–NH_2$, and –SH, which enable them to load considerably high amounts of metal ions from their dispersion medium. The electrostatic and dipole-ion attractions of the metal binding groups keep the loaded metal ions firmly affixed in the hydrogel network. The metal ions captured in hydrogel network can be readily converted into nanoparticles by chemical reduction method under mild conditions. Therefore, application of hydrogels as appropriate templates for in situ synthesis of metal nanoparticles, to prevent their aggregation and enhancing the longevity is pertinent. The larger values of both the surface energy and surface area of metal nanoparticles makes them effective catalysts for many reactions including oxidation of CO [13] nucleation of carbon nanotube [14], dehydrogenation of alcohol [15], and electro-oxidation of formic acid [16]. For example, Farooqi and coworkers prepared hydrogels bearing carboxylic groups and applied them as templates to prepare Ni and Co nanoparticles by in situ reduction within the hydrogel network [17]. These hydrogels were found as ideal templates for metal nanoparticles preparation because of their ability to act as an appropriate medium for the nucleation of nanoparticles and to avoid the agglomeration of metal nanoparticles without affecting their catalytic properties. The hydrogels containing Co and Ni nanoparticles acted as efficient catalyst in the reduction reaction of 4-nitrophenol (4-NP). Except preventing the aggregation, the hydrogels may also be helpful in tuning the catalytic properties of metal nanoparticles fabricated within their matrices. For example, the catalytic capability of the hydrogels containing nanostructured metallic particles can be varied by varying the hydrophilicity of hydrogels. In addition to variations in hydrophilicity, the variations in cross-linking density of hydrogel network also change the catalytic characteristics of nanostructured metals fabricated in hydrogels [18]. Another versatile feature of the hydrogels is that a hydrogel system can be employed as a template for the preparation of nanoparticles of many different metals or metal oxides [6, 19] which can catalyze different chemical reactions. When metal nanoparticles are fabricated in a hydrogel system then an electronic interaction is developed between the functional groups present on hydrogel network and metal nanoparticles. Therefore, once the nanoparticles of a metal are embedded in a hydrogel network, their catalytic property becomes function of the chemical nature of surrounding polymeric network. So, it is important to study the effect of various functional groups present in hydrogels on catalytic property of metal nanoparticles. In this regards, Zhang et al. prepared poly(ethylene oxide propylphosphonamidate) (PEOPPA) hydrogel and used as templates for the synthesis of nanoparticles of noble metals such as silver, platinum, gold, etc., and investigation of catalytic activity [20]. The catalysts were found to have good catalytic efficiency however the cost of noble metals and the use of toxic and expensive organic solvent THF and synthesis of hydrogel at very low temperature do not favour its applicability at large scale. Similarly, poly(sulfopropylmethacrylate) hydrogel was prepared by Sahiner et al. and nanoparticles of transition metals were embedded in this hydrogel system [21, 22]. The catalytic performance was investigated in the reduction reaction of nitrocompounds and production of hydrogen. Sahiner's group have further contributed by preparing Co nanoparticles in poly(2-acrylamido-2-methyl-1-propansulfonic acid), p(AMPS) hydrogel and investigating their catalytic properties [23]. Despite of the appreciable catalytic efficiency, the mechanism of catalytic reaction and surface analysis of the catalyst was not provided which is quite important to understand the catalytic action. To this end, we have prepared bulk hydrogel by copolymerizing acrylamide and acrylic acid and used the prepared polymeric network as a template for the fabrication of Ni nanoparticles. Fabrication of nanoparticles was accomplished by reduction of Ni(II) ions which were first entrapped in the hydrogel network from their aqueous solution. The surface analysis of catalyst was done with X-ray photoelectron spectra (XPS). Catalytic property of the prepared catalyst was investigated in the reduction of 4-NP. Effects of temperature, amount of catalyst on the reduction rate were studied. The mechanism of the catalytic reduction was also proposed.

2 Experimental work

2.1 Chemicals

Acrylamide (AAm, 98%, Merck) and acrylic acid (AAc, 99%, Alfa Aesar) were used as monomers. *N, N′*-methylene-bis-acrylamide (MBA, 99%, Sigma-Aldrich) was used a cross-linker and ammonium persulfate (APS, 99%, Sigma -Aldrich) was employed as initiator. *N, N, N′, N′*-tetramethylethylene-1,2-diamine (TEMED, 98%, Merck) was used as accelerator. Nickel chloride hexahydrate ($NiCl_2{\cdot}6H_2O$, 99%, Riedel–deHaen) was used as nickel(II) source, while sodium borohydride ($NaBH_4$, 98%, Scharlau) was employed as reducing agent. 4-NP (99%, Aldrich) was used as reductant. All the reagents were used as received from employers. Distilled water (DW) was throughout this work.

2.2 Synthesis of poly(AAm-*co*-AAc) hydrogels

Poly(AAm-*co*-AAc) hydrogel was prepared by free radical polymerization process. Total number of moles of AAc and AAm were kept as 0.028 mol. 50% of each of AAm and AAc were polymerized in the presence of 1 mol% of MBA.

A 0.5 mol% of APS was used as initiator and 1×10^{-4} L TEMED was used as accelerator. Briefly, 0.014 mol of AAm was dissolved in 1×10^{-3} L DW water in a glass vial and 0.014 mol of AAc was dissolved in DW in another glass vial. A 0.034 g (1 mol%) of MBA was dissolved in 1×10^{-3} L DW in a separate glass vial. In another glass vial, aqueous solution of APS was prepared by dissolving 0.0319 g (1 mol%) in 1 mL DW. The aqueous solutions of monomers, cross-linker and initiator were mixed together in a vial and a 1×10^{-4} L of TEMED was added as an accelerator in this reaction mixture. The reaction mixture was shaked to homogenize and then transferred to plastic straws immediately. The polymerization reaction was allowed to take place at room temperature for 24 h. After 24 h, the prepared hydrogel was taken out from plastic straws and cut into small pieces of about 5 mm length. Synthesized hydrogels were sanitized by dialysis against frequently changed DW for 3 days. After cleansing, synthesized hydrogel was placed in oven at 60 °C for drying and stored in air tight container for analysis and further use.

2.3 Fabrication of nickel nanoparticles hydrogel network

Ni nanoparticles were embedded in hydrogel networks by the reduction of Ni(II) ions within the networks of hydrogel. The preparation of Ni nanoparticles was carried out in a two steps procedure. In first step, Ni(II) ions were loaded in hydrogel. For this purpose, 0.5 g of dried poly (AAm-*co*-AAc) hydrogel was added in 250 mL, 500 ppm aqueous solution of Ni(II). Ni(II) ions were loaded by an overnight stay of hydrogels in Ni(II) solution. After Ni(II) ion loading, the hydrogel was removed from Ni(II) solution followed by removal of the loosely bound metal ions which was carried out by washing with DW. Then Ni(II) loaded hydrogel was dried in oven at 60 °C. In second step, in situ reduction of Ni(II) ions was carried out. For this purpose, 0.1 g of dried Ni(II) loaded hydrogel and 0.189 g of $NaBH_4$ were allowed to react in 50 mL DW with constant stirring at 250 rpm for 3 h. This reaction resulted in the preparation of nanoparticles of Ni in hydrogel network. The prepared hydrogel–Ni nanoparticle composite was filtered out with 2 µm pore sized plankton cloth filter paper, washed with DW water, pressed to divide the prepared composite into small pieces and employed as catalyst in the reduction reaction. For characterization, the prepared hydrogel–Ni nanoparticle composites were dried and grinded to powder form.

2.4 Characterization

Nexus 870 Fourier transform infrared spectroscopy (FT-IR) spectrometer was used to record FT-IR spectra in transmission mode of bare and composite hydrogels to identify the different functional groups. Thermal behaviour of hydrogel was investigated by thermo gravimetric analysis (TGA). TGA of prepared samples was performed on TGA Q500 V20.13 Build 39. 6–7 mg of samples was used and heating rate was kept at 10 °C/min. The thermal analysis was carried out in heat range of 40–900 °C under nitrogen atmosphere. The reduction of 4-NP was observed by measuring absorbance with UV–Vis 1601 Shimadzu spectrophotometer. X-ray diffraction (XRD) patterns were recorded by X'PRO PANalytical XRD spectrophotometer. Transmission electron microscopy (TEM) image was recorded from Tecnai G2 20 S-TWIN (200 kV LaB6) transmission electron microscope. The XPS were taken on an ESCALab MKII X-ray photoelectron spectrometer (Thermo VG Scientific, West Sussex, UK).

2.5 Catalytic action of hydrogel–nickel composite

The assessment of catalytic performance of Ni nanoparticles fabricated in hydrogel was done in a model reaction of 4-NP reduction. To a 50 mL of 10 mM aqueous solution of 4-NP, 0.0189 g of $NaBH_4$ was added as reducing agent and various amounts of p(AAm-*co*-AAc)–Ni hydrogel composite were used as catalysts. The reaction was carried in temperature controlled oil bath. For determining the progress of reaction, 0.3 mL of the reaction mixture was withdrawn after certain intervals of time, diluted with 4.2 mL DW and transferred into the quartz cell having path length equivalent to 1 cm. The UV–Vis spectra were obtained with UV–Vis spectrophotometer and decrease in concentration of 4-NP was observed from corresponding decrease in its absorbance at 400 nm with the passage of time.

3 Results and discussion

3.1 Synthesis of p(AAm-*co*-AAc) hydrogel and fabrication of Ni nanoparticles

Figure 1 represents the scheme for the synthesis of p(AAm-*co*-AAc) hydrogel and fabrication of Ni nanoparticles within the hydrogel networks. The free radical polymerization method was followed for the synthesis of p(AAm-*co*-AAc) hydrogel. The carboxylic groups of p(AAm-*co*-AAc) hydrogel networks have affinity to attract Ni(II) ions. By using this affinity, Ni(II) ions were loaded in hydrogel by immersing hydrogel in aqueous solution of Ni(II) ions. The appearance of light green colour as depicted by digital camera image (a) of Fig. 1 indicates the loading of Ni(II) ions. The Ni(II) loaded hydrogel was treated with $NaBH_4$ in aqueous medium. This reaction resulted in the formation of Ni nanoparticles that was indicated by black colour of hydrogel as depicted by digital camera image (b) in Fig. 1. The

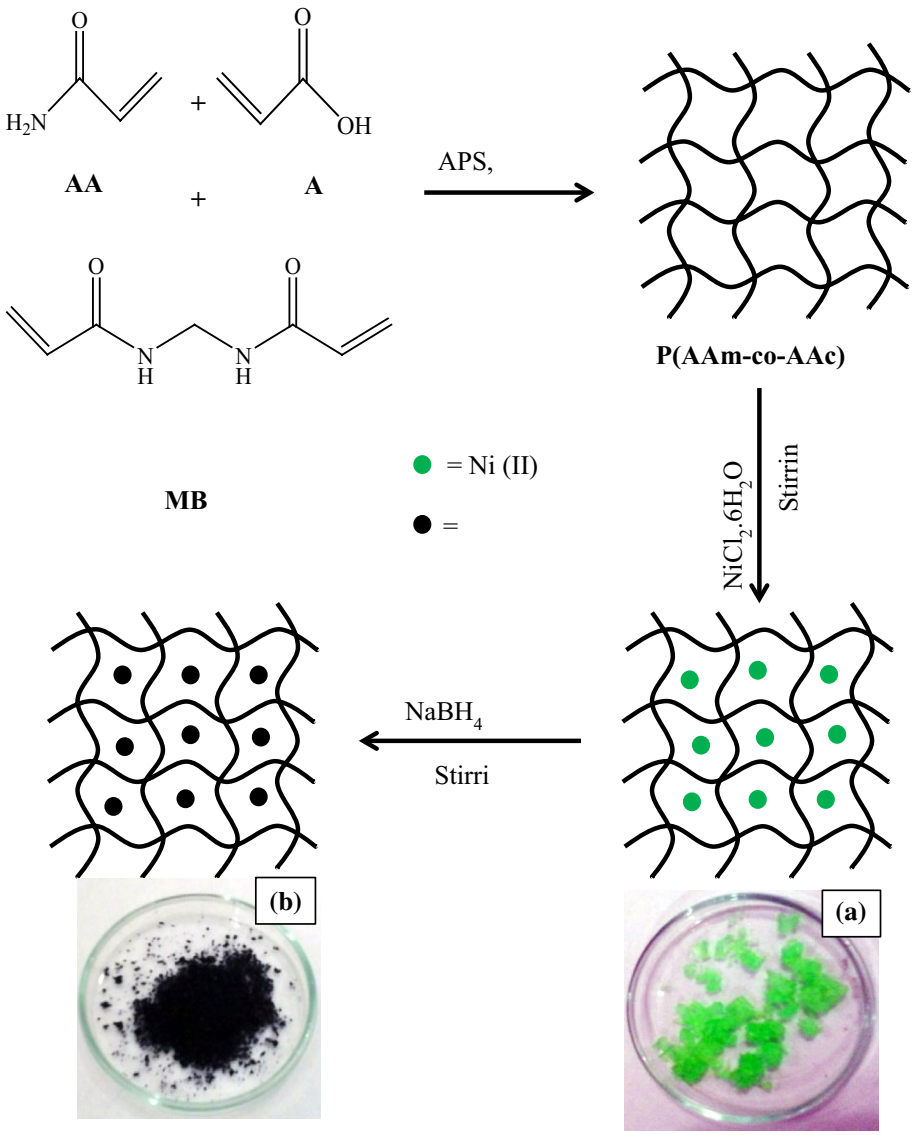

Fig. 1 Schematic representation for the synthesis of p(AAm-*co*-AAc) hydrogel and fabrication of Ni nanoparticles in p(AAm-*co*-AAc) hydrogel. The digital camera images represent the **a** Ni(II) loaded p(AAm-*co*-AAc) hydrogel and **b** p(AAm-*co*-AAc) hydrogel fabricated with Ni nanoparticles. (Color figure online)

FT-IR spectra shown in Fig. 2a indicate the development of copolymer hydrogel and the existence of metal nanoparticles inside the hydrogel. The absorption band at 3338 cm^{-1} appeared due to stretching of –OH of carboxylic acid and at 3188 cm^{-1} due to $–NH_2$ symmetric stretching of acrylamide segments. Asymmetric stretching of –CH was appeared at 2980 cm^{-1}. The absorption band at 1659 cm^{-1} was appeared due to stretching vibrations of carbonyl (C=O) groups. The absorption band corresponding to amide group was appeared at 1627 cm^{-1}. Symmetric stretching of COO^- was found at 1460 cm^{-1}. The absence of the characteristic absorption band for C=C and appearance of the absorption band corresponding to amide and carboxylic groups indicated that the monomers were polymerized and their corresponding functional groups were present in the prepared hydrogel network. XRD analysis was done for confirmation of the existence of crystalline nickel nanoparticles in the prepared copolymer hydrogel. XRD patterns of both the bare and composite hydrogel are shown in Fig. 2b. No sharp peak was exhibited by bare p(AAm-*co*-AAc) hydrogel while only a broad peak around 2θ value of 23° was attributed to polymeric network. In XRD pattern of p(AAm-*co*-AAc)–Ni hydrogel composite, the peaks appeared at 2θ values of 43°, 49° and 73° corresponds to (111), (200) and (220) planes of face centred cubic crystals of Ni, respectively. The appearance of these peaks in XRD pattern is in accordance with literature [24, 25]. The nonappearance of any sharp peak in XRD pattern of the prepared copolymer hydrogel reveals that bare hydrogel was amorphous in nature while the appearance of sharp peaks in XRD pattern of copolymer hydrogel fabricated with Ni nanoparticles reflects the incubation of crystalline material in hydrogel which are actually nickel nanoparticles. So the XRD patterns of prepared hydrogels indicate the presence of Ni nanoparticles in composite hydrogel network. Once it was

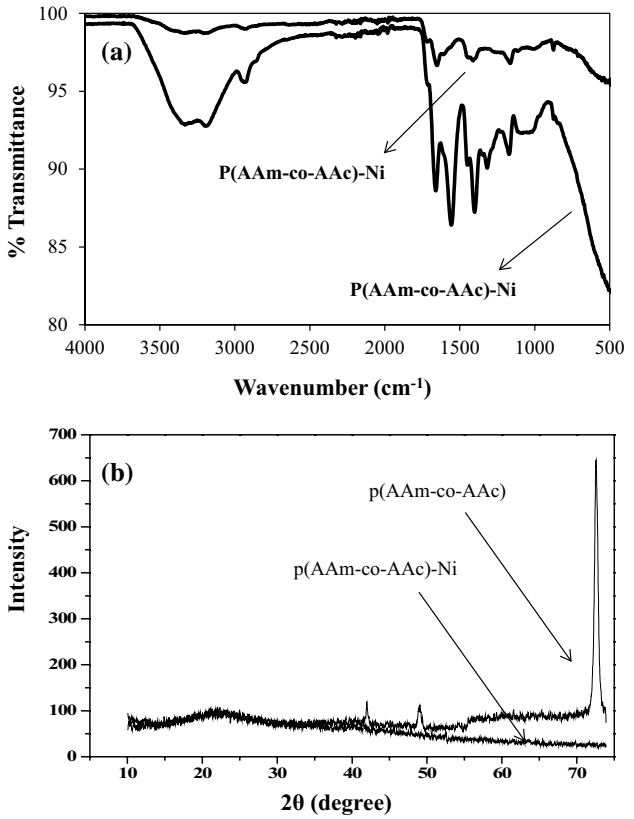

Fig. 2 **a** FT-IR spectra of p(AAm-*co*-AAc) hydrogel and p(AAm-*co*-AAc)–Ni hydrogel composite. **b** XRD patterns of p(AAm-*co*-AAc) hydrogel and p(AAm-*co*-AAc)–Ni hydrogel composite

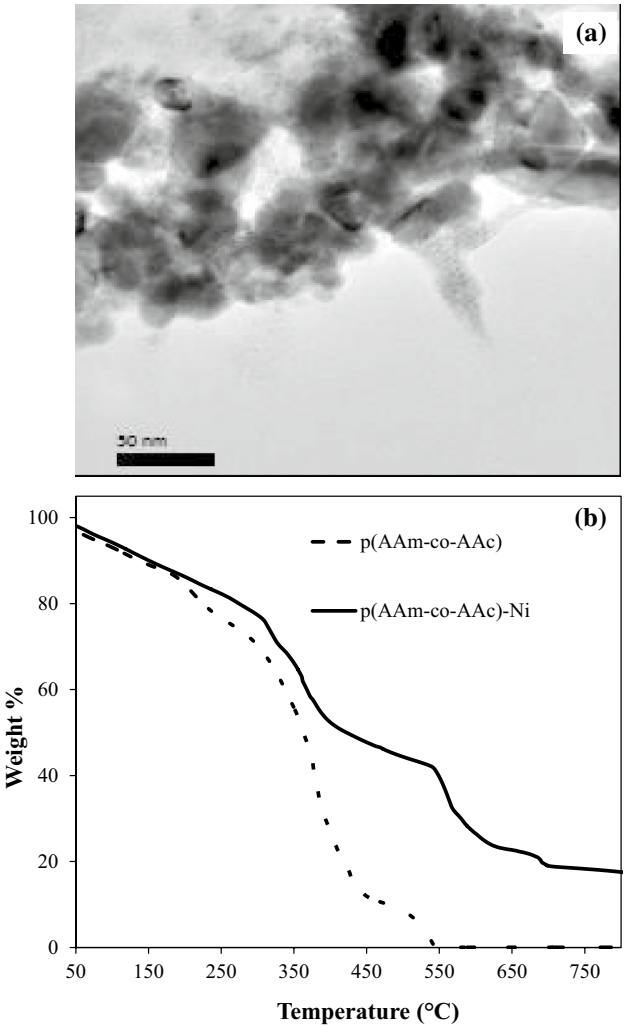

Fig. 3 **a** TEM image of Ni nanoparticles fabricated in p(AAm-*co*-AAc) hydrogel. Scale bar = 50 nm. **b** Thermogrames of p(AAm-*co*-AAc) hydrogel and p(AAm-*co*-AAc)–Ni hydrogel composite

indicated from FT-IR and XRD analysis that Ni nanoparticles were prepared in copolymer hydrogel, the Ni nanoparticles were further visualized by TEM. Figure 3a represents the TEM image of Ni nanoparticles fabricated in copolymer hydrogel. The size of Ni nanoparticles was estimated around 20 nm. The absence of aggregates in TEM image reveals that the copolymer hydrogel networks prepared in this study are suitable matrices for the in situ preparation and stabilization of Ni nanoparticles. The prevention against the aggregation of Ni nanoparticles was achieved due to cross-linked polymeric network of hydrogel. Thermal stability of the prepared bare and Ni nanoparticles containing hydrogel composite was examined with TGA. Thermogrames of bare and nickel nanoparticle embedded hydrogels are shown in Fig. 3b. As depicted from thermogrames, thermal degradation of bare hydrogel was carried out in two steps. In first step, about 80% weight loss was observed as the hydrogel was heated to 440 °C. In second step, the weight loss was reached to 95% upon heating to 540 °C. Thermograme of p(AAm-*co*-AAc)–Ni represents that fabrication of Ni nanoparticles has considerable effect on its thermal behaviour. A multistep thermal degradation of Ni–p(AAm-*co*-AAc) composite was observed with total weight losses of 24, 57 and 78% upon heating to 311, 540 and 686 °C, respectively. The total 95% weight loss was observed at 931 °C for nickel fabricated p(AAm-*co*-AAc) hydrogel composite. Difference in thermal degradations approves that after the fabrication of nickel nanoparticles in p(AAm-*co*-AAc) hydrogel, a variation in chemical structure took place. The chemical structure may undergo variations due to coordination interaction that exists between functional groups on the polymeric chain and metal nanoparticles embedded in polymeric network [26]. Since hydrogels are hydrophilic in nature and can swell by absorbing water, so determination of swelling capacity of hydrogel is very important. Virtually, all the industrial applications of hydrogels depend on this property. The presence of amide and carboxylic groups in p(AAm-*co*-AAc) hydrogel imparts hydrophilic character to this polymeric network. To study the swelling behaviour certain amount of hydrogel was immersed in DW and the hydrogel was allowed to absorb

water at room temperature. The tendency of p(AAm-*co*-AAc) hydrogel to swell by absorption of water was studied by measuring the increase in mass upon absorption of water with time. The percent swelling (% S) was determined by using following Eq. 1.

$$\% S = \frac{W_t - W_d}{W_d} \times 100, \quad (1)$$

where W_d represents the weight of dried p(AAm-*co*-AAc) hydrogel before immersing in DW, W_t represents weight of hydrogel after absorption of water at different time intervals. Figure 4 shows the percent swelling of p(AAm-*co*-AAc) hydrogel as a function of time. A maximum percent swelling of 921% was achieved in 51 h and no more increase in percent swelling was observed by further increase in time. The swelling of hydrogel by water intake can also be seen from the digital camera images of dried and swollen hydrogel pieces. The dried piece of hydrogel seems to be hard and small in size while swollen piece seems as soft and larger in size due to absorption of water.

The prepared p(AAm-*co*-AAc)–Ni hydrogel composite was also characterized with XPS to analyse the surface chemical composition. The XPS survey, O1s spectrum, Ni 2p spectrum and C1s spectrum of p(AAm-*co*-AAc)–Ni hydrogel composite are shown in Fig. 5a, b, c and d, respectively. The XPS survey demonstrates the characteristic peaks of C, O and Ni and hence confirms the presence of Ni nanoparticles in p(AAm-*co*-AAc) hydrogel. The O1s spectrum exhibits a peak at 531.41 eV which corresponds to carboxylic group in interaction with Ni nanoparticles or oxides/hydroxides might be formed during drying process [27–29]. The Ni 2p XPS spectrum reflects the characteristic peaks of Ni 2p3/2 and Ni 2p1/2 core levels at 855.8 and 873.2 eV, respectively and their corresponding satellites peaks at 862 and 880 eV, respectively [28]. The C1s spectrum shows a characteristic XPS peak of sp^2 carbon atoms peak at 285.8 eV. These sp^2 carbon atoms can be from amide or carboxyl group of the hydrogel networks. Overall, the XPS study reveals that the surface of p(AAm-*co*-AAc)–Ni composite contains the carbon and oxygen atoms containing functional groups of hydrogel networks and Ni nanoparticles.

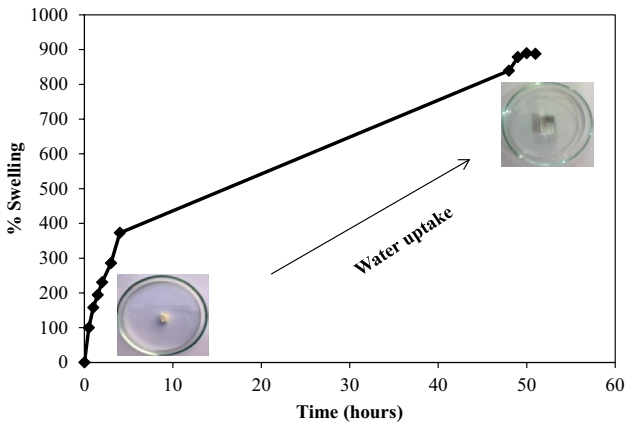

Fig. 4 The swelling percent of p(AAm-*co*-AAc) hydrogel as a function of time in distilled water

3.2 Evaluation of catalytic property

A reduction reaction involving the conversion of 4-NP to 4-AP was chosen as a model reaction to evaluate the catalytic property of synthesized copolymer hydrogel fabricated with Ni nanoparticles. In order to evaluate the catalytic property of the prepared p(AAm-*co*-AAc)–Ni hydrogel composite, In the reduction of 4-NP, $NaBH_4$ was added as a reducing agent and (AAm-*co*-AAc)–Ni hydrogel composite as a catalyst. It is worth mentioning that conversion of 4-NP to 4-AP cannot be carried out by $NaBH_4$ without aid of any catalyst [19]. Actually, this reaction is kinetically hindered due to a large kinetic barrier between mutually repelling electron donor borohydride ion (BH_4^-) and the acceptor phenolate ion ($C_6H_4NO_3^-$) [30, 31]. The presence of this kinetic barrier does not allow this reaction to take place unless a suitable catalyst is present in the reaction medium along with reactants. Therefore, this reaction is considered as an ideal reaction for the evaluation of catalytic activity of a catalyst. 4-NP is strong visible absorber having maximum absorbance wavelength (λ_{max}) at 317 nm as shown in Fig. 6a. When 4-NP is treated with $NaBH_4$ then it is converted to phenolate ion by releasing a proton and the value of λ_{max} is shifted to 400 nm as depicted by Fig. 6a. In an aqueous solution of 4-NP containing at least hundred times excess amount (w.r.t. number of moles) of $NaBH_4$, a certain amount of p(AAm-*co*-AAc)–Ni hydrogel composite was added as catalyst. The reduction of 4-NP was monitored in terms of decrease in absorbance at 400 nm after regular intervals of time. Such a decrease in absorbance is shown in Fig. 6b by UV–Vis spectra of 4-NP.

Since $NaBH_4$ was used in large excess, therefore, this reaction was considered as pseudo first order reaction. Figure 6 represents the plots of pseudo first order kinetics. Slope of the plot between $\ln(C_t/C_o)$ and time was used to measure the apparent rate constant (k_{app}). The graph of pseudo first order kinetics was plotted according to Eq. 2 [32–34].

$$\ln\left(\frac{C_t}{C_o}\right) = -k_{app}t, \quad (2)$$

where C_t represents concentration of phenolate ion at different time intervals and C_o represents initial concentration of phenolate ion. In order to calculate the activation energy, the reaction was conducted at two different temperatures and

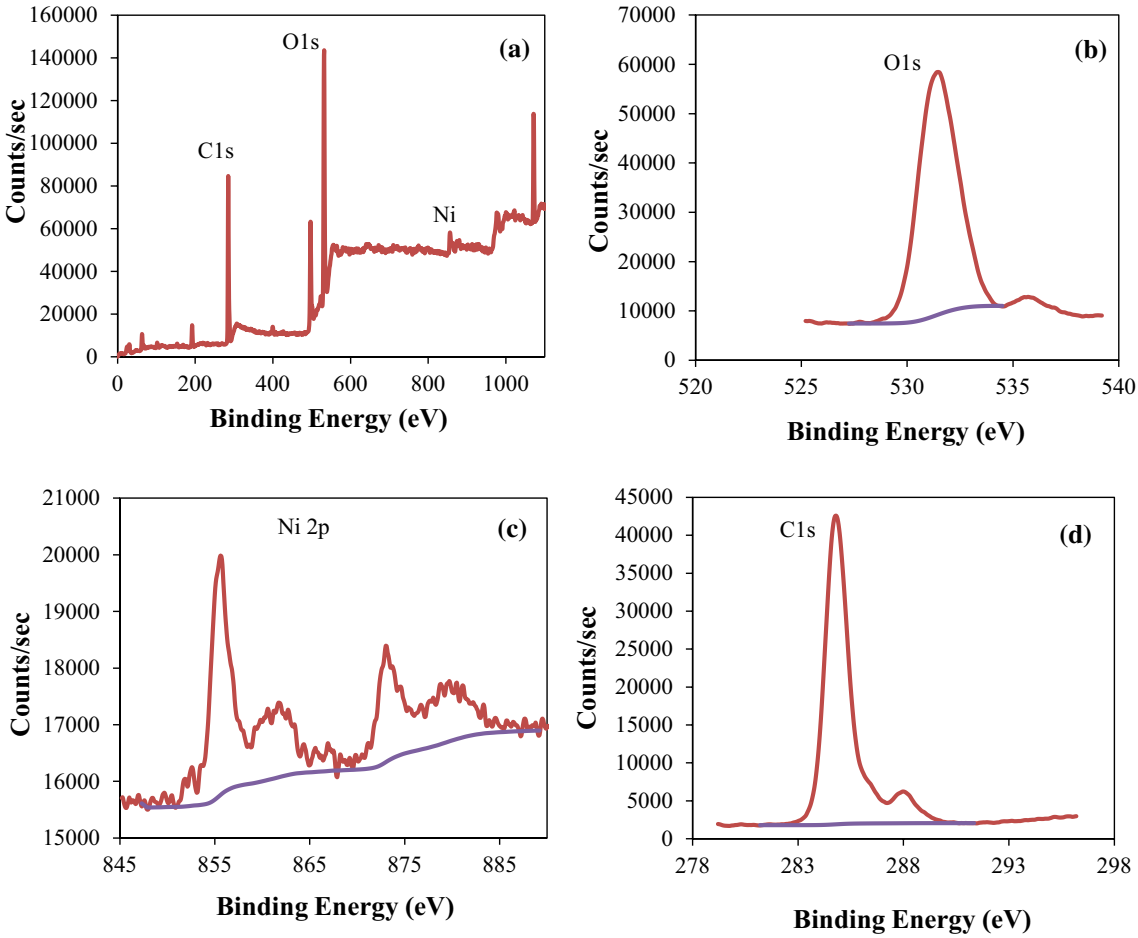

Fig. 5 The XPS survey (**a**), O1s spectrum (**b**), Ni 2p spectrum (**c**) and C1s spectrum (**d**) of Ni nanoparticles embedded in p(AAm-*co*-AAc) hydrogel

the corresponding graphs of pseudo first kinetics at different temperatures are shown in Fig. 7a. By increasing the temperature, the increase in k_{app} is depicted by bending of the plots towards horizontal axis. The k_{app} was increased from 0.085 to 0.246 min^{-1} as a consequence of an increase in temperature of the reaction medium from 30 to 50 °C. This increase in reduction rate can be achieved due to the fact that the increase in temperature raises the average kinetic energy of the reactants. As the average kinetic energy is increased the reactants colloid with higher speed which results in an increase in rate of formation of products. The activation energy for the reduction of 4-NP catalysed by p(AAm-*co*-AAc)–Ni hydrogel composite was calculated by following form of Arrhenius Eq. 3.

$$\ln\left(\frac{k_1}{k_2}\right) = \left(\frac{E_a}{R}\right)\left(\frac{T_1 - T_2}{T_1 T_2}\right), \tag{3}$$

where k_1 and k_2 are apparent rate constants at T_1 is lower temperate of reaction medium; 303 K, and T_2 is higher temperature of reaction medium; 333 K, E_a represents activation energy while R is general gas constant having value of 8.314 J/K. The value of E_a was found to be equal to 43.46 kJ/mol. The reduction of 4-NP was also carried out in the presence of four different amounts of p(AAm-*co*-AAc)–Ni hydrogel composite catalyst. All other parameters were kept constant in these reactions. An increase in the k_{app} and a decrease in time of completion of reaction were observed with the increase in catalyst dose. Figure 7b shows that k_{app} was increased from 0.09 to 0.04 min^{-1} as the amount of catalyst was increased from 0.01 to 0.07 g. Such an increase in k_{app} is attributed to the fact that with the increase in amount of catalyst the catalytic sites in reaction medium are increased. Due to availability of greater number of catalytic sites, greater numbers of reactants are adsorbed on the surface of catalyst in unit time which results in an increase in rate of formation of the products. The apparent rate constant observed in the present work is greater as compared to the recently reported (0.313 min^{-1}) by Begum et al. for the reduction of 4-NP catalysed by silver (Ag)

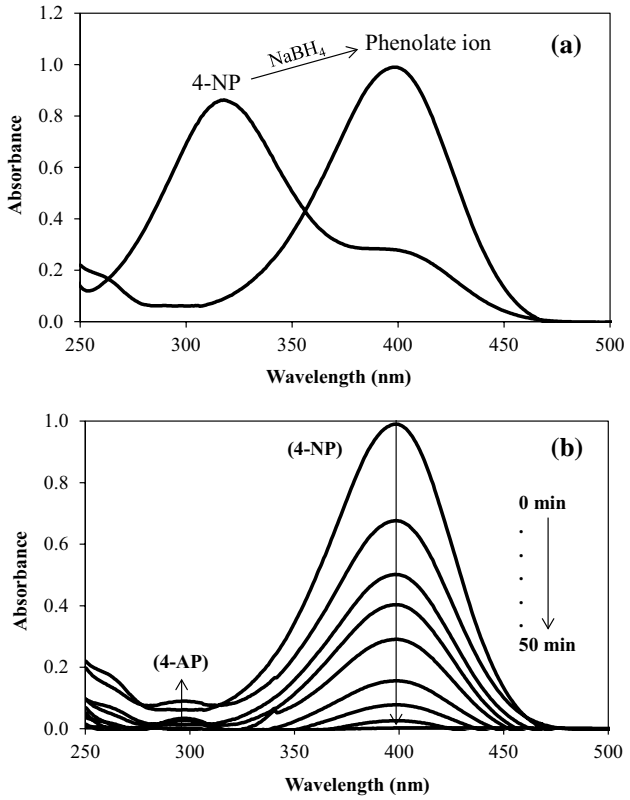

Fig. 6 UV–visible spectra for the reduction of 4-NP **a** in the absence, and **b** in the presence of p(AAm-*co*-AAc)–Ni composite (reaction conditions: 0.01 M 4-NP = 50 mL, $NaBH_4$ = 0.0189 g, 250 rpm, 30 °C)

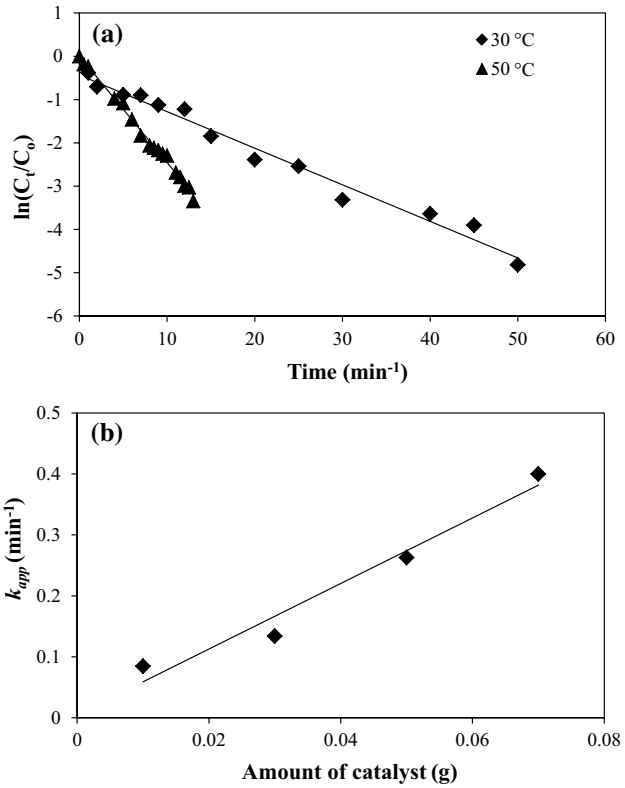

Fig. 7 **a** Plots of $\ln(C_t/C_o)$ as a function of time for the reduction of 4-NP at 30 and 50 °C. **b** Change in k_{app} with the change in amount of catalyst (reaction conditions: 0.01 M 4-NP = 50 mL, $NaBH_4$ = 0.0189 g, 250 rpm)

nanoparticles stabilized in *N*-isopropylacrylamide–acrylic acid–acrylamide microgel [35]. The apparent rate constant observed in the this work is also higher than that of cobalt nanoparticles prepared in poly(2-acrylamido-2-methyl-1-propansulfonic acid) by Sahiner et al. [23]. The catalytic activity of our prepared catalyst is also comparable with that of relatively costly Ag nanoparticles embedded in another microgel system consisting of *N*-isopropylacrylamide-2-hydroxyethylmethacrylate–acrylic acid [36]. Being a noble metal, Ag is very expensive as compared to Ni and synthesis of above mentioned *N*-isopropylacrylamide based microgels is rather difficult and energy consuming as it needs nitrogen atmosphere and high temperature condition. The higher catalytic activity can be attributed to the porous and hydrophilic nature of our hydrogel system which was used as templates for the synthesis of Ni nanoparticles. The high porosity and hydrophilic character allows rapid diffusion of reactants and products into and out of the hydrogel containing nanocatalyst. So our reported catalyst is superior as compared to recently reported catalysts used for the reduction of 4-NP in terms of its easy synthesis, cost effectiveness and catalytic activity.

According to literature reports, the reduction of 4-NP to 4-AP at the surface of a nanocatalysts takes place via Langmuir–Hinshelwood mechanism [7, 37]. The proposed mechanism for the reduction of 4-NP at the surface of Ni nanoparticle is shown diagrammatically in Fig. 8. Both the reducing agent and 4-NP react at the surface of Ni nanoparticles fabricated in hydrogel network. When $NaBH_4$ is added in water, BH_4^- is produced which is a strong nucleophile. Being a strong nucleophile, BH_4^- gives electron to catalyst and produce hydride ion. The hydride ions then react with proton (H^+) provided by water to produce hydrogen molecules (H_2). The H_2 molecules are adsorbed at the surface of Ni nanoparticles. The antibonding orbitals of the H_2 molecules accept electron pairs from electron flow of catalyst and H_2 molecules are converted into active hydrogen atoms which remain adsorbed at the surface of Ni nanoparticles. The active hydrogen atoms then attack at the nitro group of 4-NP and convert it to 4-AP via formation of intermediates containing nitroso (–NO) and hydroxylamino group (–NHOH) as shown by the structural formulas on surface of Ni nanoparticles in Fig. 8. When 4-AP is formed at the surface of Ni nanoparticles, it is desorbed from the surface of nanoparticle and in this way surface of nanoparticle is

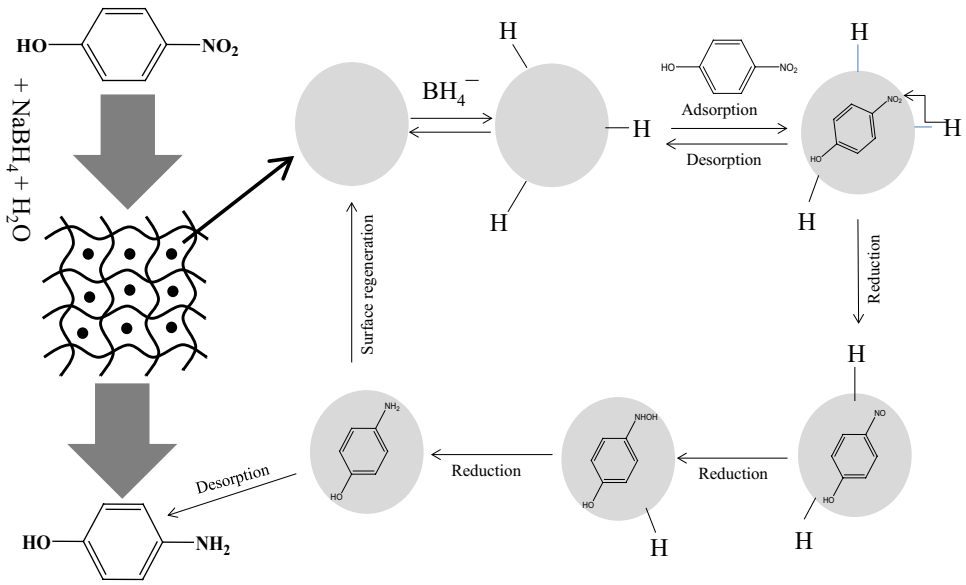

Fig. 8 Langmuir–Hinshelwood mechanism for reduction of 4-NP on the surface of Ni nanoparticles fabricated in p(AAm-*co*-AAc) hydrogel

regenerated for further action. Desorption of product is followed by the adsorption of new reactant molecules at the surface of catalyst. In this way adsorption–desorption equilibrium is established and reactants are continuously converted into the products [38]. Kinetics of such reactions depends on the rate of diffusion of reactants and products through the hydrogel network [39]. The rate of diffusion further depends on hydrophilicity of hydrogel, porosity of hydrogels and cross linking density of hydrogels. A hydrogel with high hydrophilic nature, greater porosity and low crosslinking density can facilitate easy diffusion of reactants and products and hence can be considered as suitable milieu for rapid reaction.

4 Conclusions

Synthesis of p(AAm-*co*-AAc) hydrogel was accomplished by a very simple and easy method of free radical polymerization in the presence of redox initiator and Ni nanoparticles were prepared within the hydrogel networks by in situ reduction method. FT-IR and XRD results indicated the existence of Ni nanoparticles in p(AAm-*co*-AAc) hydrogel. TGA results have shown that both the bare and composite hydrogel were stable below 200 °C and lower weight loss was observed for composite hydrogel. The rapid reduction of 4-NP in the presence of p(AAm-*co*-AAc)–Ni hydrogel composite revealed that p(AAm-*co*-AAc)–Ni hydrogel composite possess efficient catalytic property for the reduction of 4-NP. The rate of reduction was found to be the function of temperature and catalyst dose and increase in rate of reduction was observed by increasing either the temperature or catalyst dose. Activation energy (E_a) for the reduction of 4-NP was found to be 43.46 kJ/mol. A maximum reduction rate of 0.35 min^{-1} was observed at room temperature. The simple and cost effective synthesis and good catalytic results of our reported composite hydrogel catalyst reveals that these materials can be used as economical catalysts at industrials level.

Acknowledgements The Research Fund provided by the Quaid-i-Azam University (URF-2016) is highly acknowledged. We also wish to acknowledge the Higher Education Commission of Pakistan for funding under the Research Project No. 20-1468.

References

1. N. Sahiner, P. Ilgin, J. Polym. Sci. A **48**, 5239 (2010)
2. F. Brandl, F. Sommer, A. Goepferich, Biomaterials **28**, 134 (2007)
3. D. Seliktar, Science **336**, 1124 (2012)
4. G. Jing, L. Wang, H. Yu, W.A. Amer, L. Zhang, Colloids Surf. A **416**, 86 (2013)
5. H.-Q. Sun, L. Zhang, Z.-Q. Li, L. Zhang, L. Luo, S. Zhao, Soft Matter **7**, 7601 (2011)
6. J. Zhang, S. Xu, E. Kumacheva, J. Am. Chem. Soc. **126**, 7908 (2004)
7. Z.H. Farooqi, K. Naseem, R. Begum, A. Ijaz, J. Inorg. Organomet. Polym. Mater. **25**, 1554 (2015)
8. Z.H. Farooqi, T. Sakhawat, S.R. Khan, F. Kanwal, M. Usman, R. Begum, Mater. Sci. Pol. **33**, 185 (2015)
9. Z.H. Farooqi, S.R. Khan, R. Begum, A. Ijaz, Rev. Chem. Eng. **32**, 49 (2016)
10. R. Begum, K. Naseem, Z.H. Farooqi, J. Sol–Gel Sci. Technol. **77**, 497 (2016)
11. N.A. Peppas, J.Z. Hilt, A. Khademhosseini, R. Langer, Adv. Mater. **18**, 1345 (2006)
12. S. Ekici, P. Ilgin, S. Butun, N. Sahiner, Carbohydr. Polym. **84**, 1306 (2011)
13. H. Lang, S. Maldonado, K.J. Stevenson, B.D. Chandler, J. Am. Chem. Soc. **126**, 12949 (2004)
14. H. Ago, K. Murata, M. Yumura, J. Yotani, S. Uemura, Appl. Phys. Lett. **82**, 811 (2003)

15. T. Mitsudome, Y. Mikami, H. Funai, T. Mizugaki, K. Jitsukawa, K. Kaneda, Angew. Chem. **120**, 144 (2008)
16. P. Waszczuk, T.M. Barnard, C. Rice, R.I. Masel, A. Wieckowski, Electrochem. Commun. **4**, 599 (2002)
17. Z.H. Farooqi, S. Iqbal, S.R. Khan, F. Kanwal, R. Begum, e-Polymers **14**, 313 (2014)
18. Z.H. Farooqi, S.R. Khan, T. Hussain, R. Begum, K. Ejaz, S. Majeed, M. Ajmal, F. Kanwal, M. Siddiq, Korean J. Chem. Eng. **31**, 1674 (2014)
19. M. Ajmal, M. Siddiq, H. Al-Lohedan, N. Sahiner, RSC Adv. **4**, 59562 (2014)
20. L. Zhang, S. Zheng, D.E. Kang, J.Y. Shin, H. Suh, I. Kim, RSC Adv. **3**, 4692 (2013)
21. N. Sahiner, A. Kaynak, S. Butun, J. Noncryst. Solids **358**, 758 (2012)
22. T. Turhan, Y.G. Avcıbası, N. Sahiner, J. Ind. Eng. Chem. **19**, 1218 (2013)
23. N. Sahiner, H. Ozay, O. Ozay, N. Aktas, Appl. Catal. B **101**, 137 (2010)
24. A. Pandey, R. Manivannan, Recent Pat Nanomed. **5**, 33 (2015)
25. M. Tang, G. Huang, S. Zhang, Y. Liu, X. Li, X. Wang, X. Pang, H. Qiu, Mater. Chem. Phys. **145**, 418 (2014)
26. Y. Dong, Y. Ma, T. Zhai, F. Shen, Y. Zeng, H. Fu, J. Yao, Macromol. Rapid Commun. **28**, 2339 (2007)
27. S. Pisiewicz, D. Formenti, A.E. Surkus, M.M. Pohl, J. Radnik, K. Junge, C. Topf, S. Bachmann, M. Scalone, M. Beller, ChemCatChem **8**, 129 (2016)
28. P. Prieto, V. Nistor, K. Nouneh, M. Oyama, M. Abd-Lefdil, R. Díaz, Appl. Surf. Sci. **258**, 8807 (2012)
29. E. Binkauskienė, V. Jasulaitienė, A. Lugauskas, Synth. Met. **159**, 1365 (2009)
30. M. Kumar, S. Deka, ACS Appl. Mater. Interfaces **6**, 16071 (2014)
31. J. Huang, S. Vongehr, S. Tang, H. Lu, X. Meng, J. Phys. Chem. C **114**, 15005 (2010)
32. R. Begum, Z.H. Farooqi, K. Naseem, F. Ali, M. Batool, J. Xiao, A. Irfan, Crit. Rev. Anal. Chem. (2018) https://doi.org/10.1080/10408347.2018.1451299
33. Z.H. Farooqi, R. Khalid, R. Begum, U. Farooq, Q. Wu, W. Wu, M. Ajmal, A. Irfan, K. Naseem, Environ. Technol. (2018). https://doi.org/10.1080/09593330.2018.1435737
34. K. Naseem, R. Begum, W. Wu, A. Irfan, Z.H. Farooqi, Polym. Rev. **58**, 288 (2018)
35. R. Begum, Z.H. Farooqi, Z. Butt, Q. Wu, W. Wu, A. Irfan, J. Environ. Sci. (2017). https://doi.org/10.1016/j.jes.2017.12.003
36. R. Begum, K. Naseem, E. Ahmed, A. Sharif, Z.H. Farooqi, Colloids Surf. A **511**, 17 (2016)
37. R. Begum, R. Rehan, Z.H. Farooqi, Z. Butt, S. Ashraf, J. Nanopart. Res. **18**, 231 (2016)
38. Z. Farooqi, S. Khan, R. Begum, Mater. Sci. Technol. **33**, 129 (2017)
39. S.R. Khan, Z.H. Farooqi, A. Ali, R. Begum, F. Kanwal, M. Siddiq, Mater. Chem. Phys. **171**, 318 (2016)